**Supporting Information**

**Participants and Study Procedure.** Ninety-one participants (48 males) were initially recruited from the Greater Boston area, comprising 47 young adults (24 males, ages 18-35) and 44 elderly adults (24 males, ages 60-80). For all neuropsychological instruments used, participants were required to score within 1.5 standard deviations of published normative values based on their age and education. Participants arrived at the lab on Day 1 to complete a neuropsychological battery of tests, including the California Verbal Learning Test (CVLT) (1) and the Trail Making Test (TMT) (2). On Day 2 (one to three days later), participants underwent structural and resting state scans. On Day 3 (another one week later), participants completed an associative memory task (3). Paired associates consisted of 120 face-word pairs and 120 scene-word pairs. All stimuli were chosen carefully to be affectively neutral. Face stimuli were obtained from the Center for Vital Longevity Face Database (4) and depicted male and female faces from multiple age groups. Scene stimuli were obtained from the International Affective Picture System (5) and were neutral in valence and arousal. Words were selected from the Medical Research Council Psycholinguistic Database (6). All words were adjectives, selected for high frequency and high concreteness. Each image/word pair was presented for six seconds, and a total of 20 pairs (10 scene/word and 10 face/word) were encoded in a single run and a total of 4 runs were conducted. To ensure depth of encoding, participants were asked to judge whether the word 'matched' the picture. As picture/word pairs were created randomly, and pairs with an obvious semantic connection were excluded, this judgment was subjective. After a 10-minute retention delay, participants were presented with all 80 pairs learned during encoding, as well as 40 pairs made up of new words and pictures, and 40 rearranged pairs made of words and pictures seen previously, but not previously associated. Each picture was presented for six seconds, during

which time the participant responded by button press whether the pair had appeared during encoding, or whether it was a new or rearranged pair (yes/no). Each recognition trial was coded as a hit, miss, false alarm or correct rejection, and recognition accuracy was computed in terms of d', a measure which controls for individual response bias (d' = z(hits)-z(FA)). We calculated d' separately for item recognition (previously encoded pairs *vs* novel pairs) and associative recognition (previously encoded pairs *vs* rearranged pairs). Two participants were excluded from CVLT-related analyses due to missing data. One participant was excluded from recognition-related analyses due to being an outlier on item recognition score. Data and analysis scripts are available upon request.

**Within-Network Functional Connectivity and Behavioral Correlation Analyses.** *A priori* DMN and SN masks were defined in an independent sample of 89 young adults (44 men; aged 22.4±3.34) (7, 8). For details on mask creation, see (8). To explore the topography of functional connectivity in our aging sample, we generated 4mm spherical regions of interest (ROIs) in the left posterior cingulate cortex (PCC; MNI 1, -55, 17) (9) to identify the DMN and in the right dorsal anterior insula (dAI; MNI 36, 21, 1) (7) to identify the SN. We obtained Pearson's product moment correlations, *r*, between the average time course within each seed ROI and that of all voxels across the brain, converted those *r* values to *z* values using Fisher's r-to-z- transformation, and averaged the resulting *z* maps across all subjects to obtain a group map per network. Finally, we projected the group maps onto the FreeSurfer fsaverage surface. For each network, we conducted a voxel-wise two-sample t-test between superagers and typical older adults, thresholded the resulting map at $p < 0.05$ (uncorrected) and masked it by its corresponding *a priori* network mask. To identify network targets where superagers had stronger connectivity than typical older adults, we picked out gray matter peaks within the masked t-test maps and

located a voxel with the highest *z* value within each anatomical structure (Table S6). To quantify the strength of functional connectivity between seed and target regions, for all subjects in the elderly group, we created spherical ROIs (4mm) around each correlation peak and extracted the averaged time course within each ROI. We next calculated Pearson's *r* between seed and all target time courses and applied Fisher's *r*-to-*z* transformation. This resulted in one connectivity strength score per network target per subject. Finally, we calculated Pearson's *r* between each network target's connectivity strength and the 3 memory task scores (recall, item recognition and associative recognition). To correct for multiple comparisons (15 per memory test), we tested the *p*-values for significance using FDR *q* of 0.05 following the Benjamini-Hochberg procedure (10). To show specific preservation of connectivity within the DMN and SN, we selected two additional networks as control networks. Motor network seed was located in the left primary motor cortex (M1; MNI -43, -16, 42) as in (11) and visual network seed was located in the primary visual cortex (V1; MNI -19, -95, 2) as in (12). For each seed, we created a group functional connectivity map using only young adults and identified a peak in the homologous region of the right hemisphere (Table S6). Connectivity strength between each control network seed and target was calculated for all subjects in the elderly group. Finally, we also calculated Pearson's *r* between control network connectivity strength and the 3 memory task scores.

**Post-Hoc Between-Network Functional Connectivity and Behavioral Correlation Analyses.** To examine connectivity difference across networks, we masked the PCC-seeded t-test map by the SN mask and masked the dAI-seeded t-test map by the DMN mask. We observed a number of regions that showed between-network connectivity differences in superagers (Fig. S2A). Given the importance of the MCC in superaging (8, 13-15), we investigated the connectivity between the bilateral MCC and the PCC seed. We located a voxel with the highest z value within

each MCC peak (L MCC: -2, 10, 48; R MCC: 8, 14, 48) and calculated Pearson's r between its time course and the PCC time course for each subject. We conducted two-tailed planned contrasts on connectivity strength between young adults, superagers and typical older adults. We also calculated Pearson's r between connectivity strength and the 3 memory task scores (recall, item recognition and associative recognition).

**Brain-Behavior Regression Analysis.** We ran one hierarchical linear regression analysis for each index of memory as the dependent measure, using intrinsic connectivity strength between canonical network nodes as predictor variables. We picked key nodes within the DMN and SN and used their connectivity strength as predictors in each regression model. For the DMN, the predictor was PCC connectivity to the right HF; for the SN, the predictor was dAI connectivity to the left MCC connectivity. We conducted two regression analyses, one using recall as the outcome measure and the other using item recognition as outcome measure. We did not conduct an analysis for associative recognition since it was not significantly predicted by connectivity between the dAI seed and any SN target. We further ran regression analyses using neuroanatomy and functional connectivity as predictors for recall memory (CVLT). To index anatomical preservation, we initially planned to include cortical thickness/volume estimates for the regions used to compute estimates of intrinsic connectivity (i.e. R HF and R PCC for the DMN, L MCC and R dAI for the SN). R PCC thickness was not preserved in superagers (8) and R dAI thickness was not independently associated with CVLT performance over and above R HF volume and L MCC thickness, and so we excluded R PCC and R dAI from the analyses. As a consequence, we ran two regression analyses to predict CVLT performance, one using R HF volume and R HF-R PCC connectivity as DMN predictors, and the other using L MCC thickness and L MCC-R dAI connectivity as SN predictors, respectively. The structural data were

calculated based on the HF and MCC labels from (8). Then we ran one additional regression analysis with anatomical and functional variables of both networks as predictors. Cortical thickness measures did not significantly predict item recognition memory or associative recognition memory so additional regression analyses were not necessary in that regard. For all above tested hierarchical regression models, we further added LMCC-R PCC connectivity strength as an index for between-network connectivity to test whether it uniquely contributed to memory.

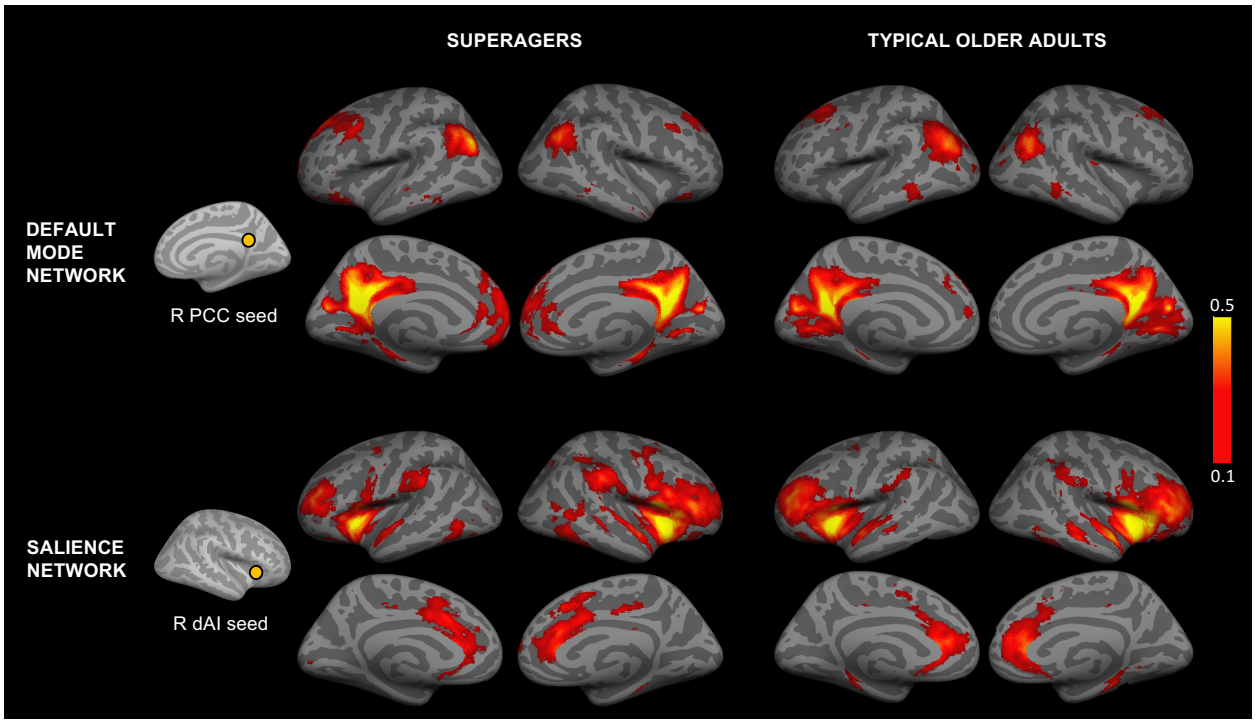


Figure S1. Spatial topography of the DMN and SN in both elderly groups. Network seed regions are indicated by orange circles. Group-averaged heat maps were thresholded at $z > 0.1$.

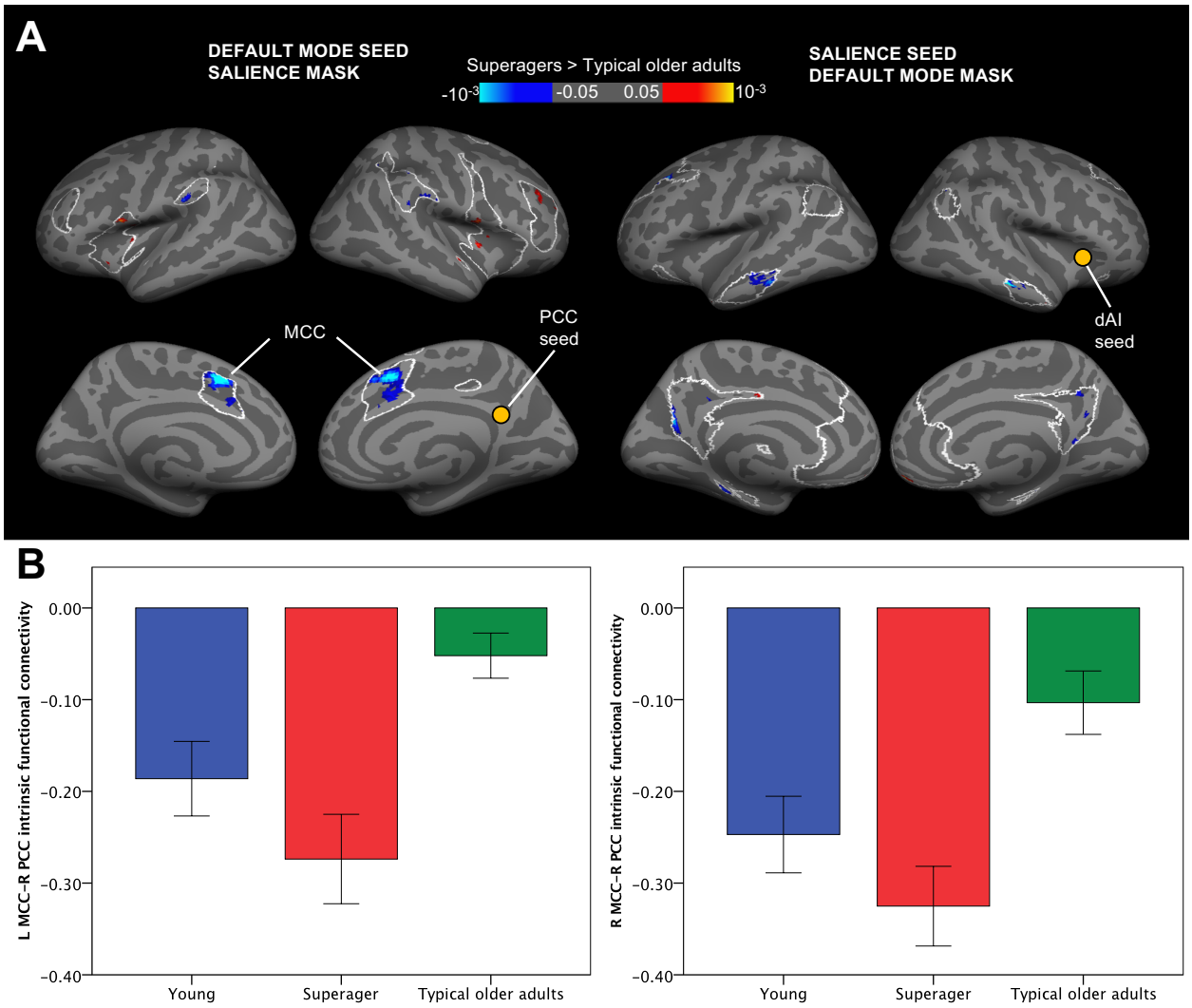


Figure S2. Between-network connectivity differences. A) Regions of the DMN and SN (outlined in white) where superagers had higher between-network connectivity (red/yellow) or lower between-network connectivity (blue-cyan) than did typical older adults. Notably, bilateral MCC, a key superaging region consistently showing anatomical preservation across multiple studies (8, 13-15), was more strongly inversely correlated with the PCC seed in superagers compared to typical older adults. Other regions showing group differences include bilateral SMG, right MFG, and bilateral mid insula from the SN, as well as bilateral MTG and PCC from the DMN. For each network, a two-sample t-test between superagers and typical older adults was conducted. Maps were thresholded at $p < 0.05$ and masked by the opposite network. B) Bar graphs show that in superagers and young adults, the MCC was more strongly inversely correlated with PCC compared to typical older adults ($p < 0.05$). There was no difference in MCC-PCC connectivity strength between superagers and young adults. We calculated intrinsic connectivity strength between the right PCC seed and bilateral MCC targets identified from peaks in the t-test maps in panel A. R, right hemisphere; L, left hemisphere. Error bars indicate 1 standard error of the mean.

Table S1. Association between memory and intrinsic connectivity between DMN and SN

| Target-Seed | Recall | | Recognition Item | | Recognition Associative | |
|---|---|---|---|---|---|---|
| | *r* | *p* | *r* | *p* | *r* | *p* |
| L MCC-R PCC | -0.393 | 0.007** | -0.445 | 0.002** | -0.355 | 0.013* |
| R MCC-R PCC | -0.472 | 0.001** | -0.167 | 0.154 | -0.076 | 0.323 |

Note: $r$ = Pearson's correlation coefficients, $p$ = one-tailed significance. Uncorrected significance: * $p < 0.05$, ** $p < 0.01$.

Table S2. Stronger functional connectivity in the DMN and in the SN independently predicted better item recognition memory performance in the elderly group.

| | Item recognition memory performance | | | |
|---|---|---|---|---|
| | *B* | *t* | $R^2$ change | Total $R^2$ |
| R HF-R PCC connectivity[a] | 0.26 | 1.71 | 0.07 | 0.15 |
| L MCC-R dAI connectivity[b] | 0.28 | 1.79 | 0.08 | |

Note: This table displays standardized regression coefficient (*B*), t statistic (*t*), incremental variance ($R^2$ change), as well as total variance (Total $R^2$) in item recognition memory performance predicted by entering both independent variables into a single multiple linear regression model. Incremental $R^2$ change indicates additional variance explained by respective independent variable when entered last in the model. [a]$p = 0.096$, [b]$p = 0.082$.

Table S3. Stronger functional connectivity between the DMN and in the SN independently predicted better item recognition memory performance in the elderly group.

| | Item recognition memory performance | | | |
|---|---|---|---|---|
| | *B* | *t* | $R^2$ change | Total $R^2$ |
| R HF-R PCC connectivity[a] | 0.10 | 0.62 | 0.01 | 0.26 |
| L MCC-R dAI connectivity[b] | 0.23 | 1.56 | 0.05 | |
| L MCC-R PCC connectivity[c] | -0.37 | -2.26 | 0.11 | |

Note: This table displays standardized regression coefficient (*B*), t statistic (*t*), incremental variance ($R^2$ change), as well as total variance (Total $R^2$) in item recognition memory performance predicted by entering both independent variables into a single multiple linear regression model. Incremental $R^2$ change indicates additional variance explained by respective independent variable when entered last in the model. [a]$p = 0.54$, [b]$p = 0.13$, [c]$p = 0.03$.

Table S4. Combining both DMN and SN, higher structural integrity and stronger functional connectivity independently predicted better recall memory performance in the elderly group.

| | Recall memory performance | | | |
|---|---|---|---|---|
| | *B* | *t* | $R^2$ change | Total $R^2$ |
| Structural variables[a] | | | | |
| Adjusted R hippocampal volume[c] | 0.35 | 2.60 | 0.15 | 0.44 |
| Adjusted L MCC thickness[d] | 0.21 | 1.48 | | |
| Functional variables[b] | | | | |
| R HF-R PCC connectivity[e] | 0.22 | 1.63 | 0.13 | |
| L MCC-R dAI connectivity[f] | 0.31 | 2.26 | | |

Note: This table displays standardized regression coefficient (*B*), t statistic (*t*), incremental variance ($R^2$ change), as well as total variance (Total $R^2$) in recall memory performance predicted by entering both independent variables into a single multiple linear regression model. Incremental $R^2$ change indicates additional variance explained by respective block of independent variables when entered last in the model. p values for each block of variables: [a]p = 0.019, [b]p = 0.033. p values for each independent variable: [c]p = 0.014, [d]p = 0.149, [e]p = 0.114, [f]p = 0.031.

Table S5. List of tasks completed by participants in chronological order.

| |
|---|
| **Day 1** |
| Flanker |
| Continuous Performance Task |
| 1-Back and 2-Back |
| Affective Reactivity Task |
| Heartbeat Detection Task |
| Continuous Flash Suppression |
| **CVLT start** |
| **Demographics** |
| Handedness |
| Mini-Mental State Examination |
| Questionnaires (GAI, STAI, NEO, AMNART, SES, BDI) |
| **CVLT end** |
| Puzzles |
| Verbal Fluency |
| Category Fluency |
| Social Network Index |
| **Day 2** |
| **Trail Making Test** |
| **Structural scan** |
| **Resting state scan** |
| Recognition memory task under negative mood induction |
| **Day 3** |
| Trail Making Test |
| Structural scan |
| Resting state scan |
| **Recognition memory task under neutral mood induction** |

Tasks analyzed for the current study are bolded.

Table S6. MNI coordinates of seed and target regions within the default mode, salience and motor networks.

| Region | MNI coordinates | | |
|---|---|---|---|
| | x | y | z |
| Default mode network | | | |
| PCC seed | 1 | -55 | 17 |

| | | | |
|---|---|---|---|
| L AG | -42 | -74 | 50 |
| L SFG | -16 | 37 | 40 |
| L dmPFC | -1 | 55 | 15 |
| L rmPFC | -4 | 56 | -13 |
| R AG | 54 | -57 | 42 |
| R aMTG | 61 | 5 | -29 |
| R vlPFC | 35 | 34 | -16 |
| R dmPFC | 9 | 54 | 19 |
| R pgACC | 5 | 31 | 12 |
| R sgACC | 5 | 34 | -1 |
| R rmPFC | 9 | 46 | -6 |
| R HF | 27 | -22 | -18 |
| Salience network | | | |
| dAI seed | 36 | 21 | 1 |
| L MCC | -1 | 14 | 28 |
| R MCC | 3 | 6 | 34 |
| R SMG | 56 | -25 | 37 |
| Motor network | | | |
| L M1 seed | -28 | -28 | 53 |
| R M1 | 33 | -29 | 54 |
| L V1 seed | -19 | -98 | -3 |
| R V1 | 19 | -101 | -2 |


1. Delis DC, Kramer JH, Kaplan E, & Ober BA (1987) *California verbal learning test, research edition, manual.* (The Psychological Corporation, Harcourt Brace Jovanovich, San Antonio).
2. Tombaugh TN (2004) Trail Making Test A and B: Normative data stratified by age and education. *Archives of Clinical Neuropsychology* 19(2):203-214.
3. Andreano JM, Touroutoglou A, Dickerson BC, & Feldman Barrett L (2017) Resting Connectivity Between Salience Nodes Predicts Recognition Memory. *Soc Cogn Affect Neurosci*.
4. Minear M & Park DC (2004) A lifespan database of adult facial stimuli. *Behav Res Methods Instrum Comput* 36(4):630-633.
5. Lang PJ, Bradley MM, & Cuthbert BN (1997) *International Affective Picture System (IAPS): Technical Manual and Affective Ratings.* (NIMH Center for the Study of Emotion and Attention, Gainesville, FL).
6. Coltheart M (1981) The MRC Psycholinguistic Database. *Quarterly Journal of Experimental Psychology* 33(A):497-505.

7. Touroutoglou A, Hollenbeck M, Dickerson BC, & Feldman Barrett L (2012) Dissociable large-scale networks anchored in the right anterior insula subserve affective experience and attention. *NeuroImage* 60(4):1947-1958.
8. Sun FW*, et al.* (2016) Youthful Brains in Older Adults: Preserved Neuroanatomy in the Default Mode and Salience Networks Contributes to Youthful Memory in Superaging. *The Journal of neuroscience : the official journal of the Society for Neuroscience* 36(37):9659-9668.
9. Vincent JL, Kahn I, Snyder AZ, Raichle ME, & Buckner RL (2008) Evidence for a Frontoparietal Control System Revealed by Intrinsic Functional Connectivity. *Journal of Neurophysiology* 100(6):3328-3342.
10. Benjamini Y & Hochberg Y (1995) Controlling the false discovery rate: a practical and powerful approach to multiple testing. *Journal of the royal statistical society. Series B (Methodological)*:289-300.
11. Andoh J, Matsushita R, & Zatorre RJ (2015) Asymmetric Interhemispheric Transfer in the Auditory Network: Evidence from TMS, Resting-State fMRI, and Diffusion Imaging. *The Journal of neuroscience : the official journal of the Society for Neuroscience* 35(43):14602-14611.
12. Konishi S, Wheeler ME, Donaldson DI, & Buckner RL (2000) Neural correlates of episodic retrieval success. *Neuroimage* 12(3):276-286.
13. Rogalski EJ*, et al.* (2013) Youthful Memory Capacity in Old Brains: Anatomic and Genetic Clues from the Northwestern SuperAging Project. *Journal of Cognitive Neuroscience* 25(1):29-36.
14. Harrison TM, Weintraub S, Mesulam MM, & Rogalski E (2012) Superior Memory and Higher Cortical Volumes in Unusually Successful Cognitive Aging. *Journal of the International Neuropsychological Society* 18(06):1081-1085.
15. Gefen T*, et al.* (2014) Longitudinal Neuropsychological Performance of Cognitive SuperAgers. *Journal of the American Geriatrics Society* 62(8):1598-1600.